

# (n,xn) cross section measurements for Y-89 foils used as detectors for high energy neutron measurements in the deeply subcritical assembly “QUINTA”

Marcin Bielewicz<sup>1,2,a</sup>, Stanisław Kilim<sup>1</sup>, Elżbieta Strugalska-Gola<sup>1</sup>, Marcin Szuta<sup>1</sup>, Andrzej Wojciechowski<sup>1,2</sup>, Sergey Tyutyunnikov<sup>2</sup>, Alexander Prokofiev<sup>3</sup>, and Elke Passoth<sup>3</sup>

<sup>1</sup> National Centre for Nuclear Research, Otwock-Świerk 05-400, Poland

<sup>2</sup> Joint Institute for Nuclear Research, 141980 Dubna, Russia

<sup>3</sup> Uppsala University, Box 516, 751 20 Uppsala, Sweden

**Abstract.** Study of the deep subcritical systems (QUINTA) using relativistic beams is performed within the project “Energy and Transmutation of Radioactive Wastes” (E&T – RAW). The experiment assembly was irradiated by deuteron/proton beam (Dubna NUCLOTRON). We calculated the neutron energy spectrum inside the whole assembly by using threshold energy (n,xn) reactions in yttrium (Y-89) foils. There are almost no experimental cross section data for those reactions. New Y-89(n,xn) cross section measurements were carried out at The Svedberg laboratory (TSL) in Uppsala, Sweden in 2015. In this paper we present preliminary results of those experiments.

## 1. Introduction and motivation

Our work is a preliminary step in the study of physical and geometrical properties of future ADS systems. A very deeply subcritical active core made of natural uranium (QUINTA assembly) was irradiated by pulsed beams of relativistic particles (protons, deuterons or carbon ions) with energies in 0.5–24 GeV range, extracted from Dubna accelerators [1,2]. The long-term goal is to study the possibilities of using such systems with maximal hard neutron spectrum for transmutation of radioactive wastes (RAW).

We have begun with an experimental study of neutron spectra at various locations in the volume of the QUINTA assembly (Fig. 1).

A new “ready to use” assembly QUINTA, located at the Joint Institute for Nuclear Research (JINR), Dubna, Russia, has been used by the E&T RAW collaboration since 2010. The QUINTA assembly is made of 512 kg of natural uranium. The assembly consists of five sections, each 114 mm long, separated by 17-mm air gaps that allow us to place activation samples mounted onto special plates (Fig. 1). The uranium is presented by cylindrical rods (61 rods in each section), each rod is 36 mm in diameter, 104 mm long and 1.72 kg weight. The first section contains only 54 rods, which leave space for a beam window. The QUINTA assembly, weighting in total 1780 kg, is mounted onto a single aluminum plate with the thickness of 25 mm and surrounded by 100-mm thick lead bricks from all the six sides. The frontal side of the lead bunker has a square-shaped window, 150 × 150 mm.

<sup>89</sup>Y activation foils with chemical purity > 99.99% were placed inside the QUINTA assembly on the detector

plates. After irradiation the samples were analyzed using  $\gamma$ -spectrometer based on a HPGe n-type coaxial detector. The obtained  $\gamma$ -spectra were analyzed using the DEIMOS [3] program. Using this program we performed energy calibrations and determined absolute intensity of the observed peaks in the spectrum, Full Width at Half Maximum (FWHM), and respective errors. Finally, basing on Table 1 data we obtained the number of produced nuclei of each analyzed isotope  $N$  using the following formula (1). Spatial distributions of <sup>88</sup>Y, <sup>87</sup>Y, <sup>86</sup>Y and <sup>85</sup>Y isotope production in the QUINTA assembly were measured. Errors in the spatial distributions of isotope production are 10-20%, dependent on the location.

$$N = \frac{P}{I_{\gamma} \cdot \varepsilon_p \cdot COI} \cdot \frac{t_{real}}{t_{live}} \cdot \frac{\lambda \cdot t_{irr}}{[1 - \exp(-\lambda \cdot t_{irr})]} \cdot \frac{\exp(\lambda \cdot t_+)}{[1 - \exp(-\lambda \cdot t_{real})]} \quad (1)$$

Where:  $N$  number of produced nuclei  
 $P$  is the peak area (the number of counts),  
 $I_{\gamma}$  is the absolute intensity of the given line,  
 $\varepsilon_p(E)$  is the detector efficiency as a function of energy,  
 $COI(E,G)$  is the cascade effect coefficient as a function of energy and geometry,  
 $T_{1/2}$  is the half life time (s),  
 $t_{irr}$  is the elapsed time of the irradiation (s),  
 $t_+$  is the elapsed time from the end of the irradiation to the beginning of the measurement (s),  
 $t_{real}$  is the elapsed time of the measurement (s),  
 $t_{live}$  is the “live” time of the measurement (s),  
 $\lambda$  is the decay constant.

Having determined isotope production at specified positions in the QUINTA assembly for the three isotopes

<sup>a</sup> e-mail: marcin.bielewicz@ncbj.gov.pl

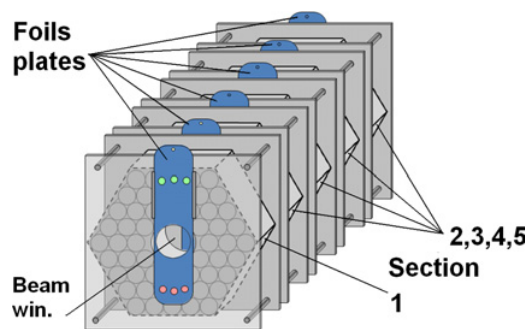


**Figure 1.** A schematic layout of the QUINTA uranium target with supporting structures and with six metallic foils plates (blue) used for sample placement [2].

**Table 1.**  $^{89}\text{Y}(n,xn)$  reaction basic data.

Reaction	T1/2	Thr. E [MeV]	$E_{\gamma}$ [keV]	$I_{\gamma}$	COI
$^{89}\text{Y}(n,2n)^{88}\text{Y}$	106.65d	11.5	898.042	0.937	1
			1836.063	0.992	1
$^{89}\text{Y}(n,3n)^{87m}\text{Y}$	13.37h	20.8	380.79	0.78	1
$^{89}\text{Y}(n,3n)^{87}\text{Y}$	79.8h	20.8	388.53	0.82	0.876
			484.805	0.897	0.878
$^{89}\text{Y}(n,4n)^{86}\text{Y}$	14.74h	32.7	1076.64	0.82	0.834

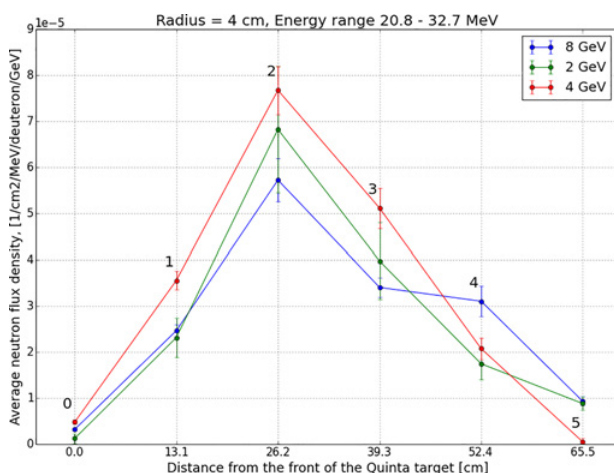


**Figure 2.** Average neutron flux density per deuteron and its energy as a function of the axial position in the QUINTA target at the radius of 4 cm, for three deuteron energies (2, 4, 8 GeV) in the neutron energy range (20.8–32.7 MeV). (A note for readers black-and-white – In position “2” (26,2 cm), the upper “red” line correspond to the incident energy of 4 GeV, the medium “green” line to 2 GeV, lower “blue” line to 8 GeV.)

$^{88}\text{Y}$ ,  $^{87}\text{Y}$  and  $^{86}\text{Y}$ , and knowing energy thresholds for the respective (n,xn) reactions, we can estimate average high-energy neutron flux in three energy ranges from 11 to 100 MeV in each  $^{89}\text{Y}$  foil’s location [4,5]. In Fig. 2 we present an example of results for the average neutron flux density in the energy range 20.8–32.7 MeV per deuteron and per unit incident deuteron energy, for different location inside the QUINTA assembly. The results are compared for three different deuteron beam irradiations performed in Dec. 2012, with the energies of 2, 4, and 8 GeV.

In order to estimate the high energy neutron field, we need to know the microscopic cross sections for the  $^{89}\text{Y}(n,xn)$  reactions. We can retrieve some cross-section data for the reactions from the EXFOR data

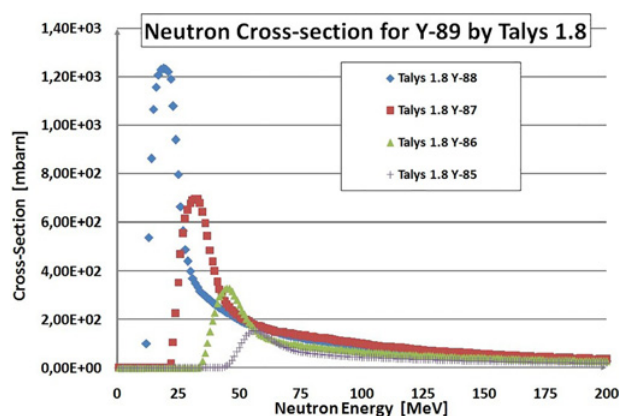


**Figure 3.** Microscopic cross sections calculated by TALYS 1.8 code for  $^{89}\text{Y}(n, xn)$  reactions [9].

**Table 2.** Beam and Calculation Parameters.

Proton Energy	38 MeV	50 MeV
Neutron Energy Peak (calc.)	35.5 MeV	47.5 MeV
Thickness of Li-7 target	4 mm	4 mm
Beam Current	5050 nA	5050 nA
Fraction of neutrons in the Peak (calc.)	21.6%	25.7%
Peak Neutron Fluence (calc.)	3.52E+10	5.39E+10
BCF for Y-88 isotope	0.21	0.18
BCF for Y-87 isotope	0.79	0.36
BCF for Y-86 isotope	1.00	0.92
Beam instability correction	1.2	1.0

base [6]. Unfortunately, the volume of the available data is insufficient, except for the cross section of the  $^{89}\text{Y}(n, 2n)$  reaction. We have not found sufficient data for the other studied reactions for neutron energies higher than 30–40 MeV. This is the reason why our cross sections were calculated using the TALYS code [7] (Fig. 3).

The Yttrium foils have the following advantages: one stable isotope ( $^{89}\text{Y}$ ), several threshold reaction channels, and several resulting isotopes with sufficiently long half-life time (longer than 12 hours). It was our motivation to make experiments to measure cross-section values for those (n,xn) reactions. New experiments for the  $^{89}\text{Y}$  cross section measurements were carried out at TSL in Uppsala [8] in 2015. Here is our first and preliminary results from those experiments.

## 2. Cross-section measurement

In 2015 we performed 4 experiments at the quasi-monoenergetic neutron (QMN) facility [8] in TSL with four different peak neutron energies (see Table 2 for the actual beam parameters). Neutrons were produced by a proton beam accelerated in the cyclotron, incoming to a  $^7\text{Li}$  target. Protons that did not react with  $^7\text{Li}$  nuclei were deflected by magnetic field and guided to the dumping line, which ended at the beam dump far away from the experimental area. After passing the magnet area and the end-window of the vacuum system, a pure quasi-monochromatic neutron beam arrived at our  $^{89}\text{Y}$  foils,

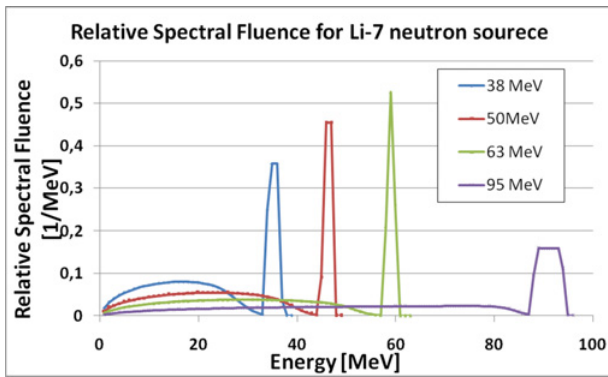


**Figure 4.** Relative spectral fluence of quasi-monochromatic neutrons with peak energies of 37.9, 48.8, 61.3, and 95.5 MeV at 0° angle, calculated according to the algorithm from [11] and normalized so that the peak area is unity. The <sup>7</sup>Li target thickness amounted to 4 mm, except for the irradiation with neutron energy of 95.5 MeV, for which the target was 23.5 mm thick [11].

located at the distance 198 cm from the <sup>7</sup>Li target, in so-called Close User Position (CUP) [9].

First step in the procedure of determination of the studied cross section was  $\gamma$ -measurement, which allowed us to determine the number of produced nuclei  $N$  in our <sup>89</sup>Y foils using Eq. (1).

As reaction <sup>89</sup>Y(n,3n) has two channels, the ground one ( $T_{1/2} = 79.8$ h) and the isomeric one ( $T_{1/2} = 13.37$ h) more complicated formula, accounting for decay scheme effect, was used for total cross section determination.

In case of reaction <sup>89</sup>Y(n,4n) the decay scheme effect ( $T_{1/2} = 14.74$ h and 47.7m) was neglected.

The main contribution to uncertainties (3–20%) in the experimental results are due to peak area determinations and statistical errors coming from the DEIMOS program [3]. The other corrections contributed with errors in the range of about 1–3%. Furthermore, there are uncertainties in the measurements that involve the total number of the primary protons in each experiment. We estimate that the overall uncertainties of the experimental data are 15–25%.

The QMN facility at TSL [8], based on the <sup>7</sup>Li(p,n) reaction, provides neutron beams with spectra comprising the high-energy peak and the low-energy tail (see Fig. 4), with approximately equal fractions in the neutron spectrum. This feature of the neutron beams necessitates the second step in the data processing, namely the determination of the background correction factor (BCF), which we define as the ratio between the numbers of nuclei produced by the high-energy peak and by the whole neutron spectrum (high-energy peak plus low-energy tail). Only in case when the threshold energy point is close (on the left) to the high-energy peak, the neutron tail background is insignificant. In this case correction factor will be close to unity. In other cases, we have determined the correction factor using the procedure from [10]. We can express the BCF by the following formula:

$$BCF = \frac{\sum_{i \in Peak} \sigma_i \cdot N_i}{\sum_i \sigma_i \cdot N_i} \quad (2)$$

where  $\sigma_i$  is binned cross section of the studied (n,xn) reaction and  $N_i$  is binned relative spectral fluence (both

**Table 3.** <sup>89</sup>Y (n,xn) cross-section measurement results.

Proton Energy	38 MeV	50 MeV
Neutron Energy		
Peak (calc.)	35.5 MeV	47.5 MeV
<sup>89</sup> Y(n,2n) <sup>88</sup> Y	103 (31) mbarn	95 (28) mbarn
<sup>89</sup> Y(n,3n) <sup>87</sup> Y	319 (64) mbarn	198 (40) mbarn
<sup>89</sup> Y(n,4n) <sup>86</sup> Y	338 (68) mbarn	132 (26) mbarn

with energy step 1 MeV). This formula was transformed from integration to summation because neutron spectrum and cross section values are binned. The procedure for the determination of the BCF is independent of the absolute values of the cross section. It depends only on the shape of the excitation function. Consequently we have been able to determine the BCF using the relative spectral fluence data calculated according to the algorithm from [11] (see Fig. 4). We have estimated the overall uncertainty brought in by BCF procedure to be approximately 10% [12]. Results of the BCF calculation are shown in Table 2.

Third step is determination of the studied cross section according to the following formula [10]:

$$\sigma = N \cdot BCF \cdot \frac{S \cdot A \cdot B_{cor}}{N_n \cdot N_A \cdot m} \cdot 10^{24} \quad (3)$$

where  $\sigma$  is the cross section for the studied (n,xn) reaction for the average energy in the high-energy peak (mb),  $S$  is the foil (detector) area (cm<sup>2</sup>),  $A$  is the molar mass of the foil material (g),  $B_{cor}$  is the beam instability correction,  $N_n$  – is the number of neutrons in the high-energy peak,  $N_A$  is the Avogadro’s number,  $m$  is the foil (detector) mass (g).

For the calculation of the  $N_n$  value we used our own MCNPX calculation for simulation of conditions at the QMN facility at TSL (MCNPX ver. 2.7.0 with tabulated values of cross-section ENDF.80c and 3007.00h Los Alamos library (2000) for Li-7 proton reactions). The proton beam current value just upstream of the <sup>7</sup>Li target was assumed to be 5050 nA.

### 3. Cross-section results and conclusion

In this paper we present preliminary results for two of our four experiments, namely for those with the proton energies of  $\approx 38$  and 50 MeV. These results are preliminary because we still need to analyze and compare neutron fluence data coming from our own calculation with the data that we are to receive from the TSL. Additionally we need to continue analyzing cross-section table for the reaction <sup>7</sup>Li(p,n) reaction, especially for energies higher than 40–50 MeV. This data table has problems, according to [11].

Finally we have calculated cross-section values for two neutron energies and for three (n,xn) reactions, <sup>89</sup>Y(n,2n)<sup>88</sup>Y, <sup>89</sup>Y(n,3n)<sup>87</sup>Y and <sup>89</sup>Y(n,4n)<sup>86</sup>Y. The errors are at least 20–30%. The results are given in Table 3 and in Fig. 5, which includes also comparisons of our experimental data with TALYS 1.8 calculations.

As pointed out earlier, for the <sup>89</sup>Y(n,2n)<sup>88</sup>Y reaction there are abundant experimental data in the EXFOR database, however only for energies up to 35 MeV. For the <sup>89</sup>Y(n,3n)<sup>87</sup>Y reaction there are several data sets for lower and higher energy (see Fig. 6). Finally, for the

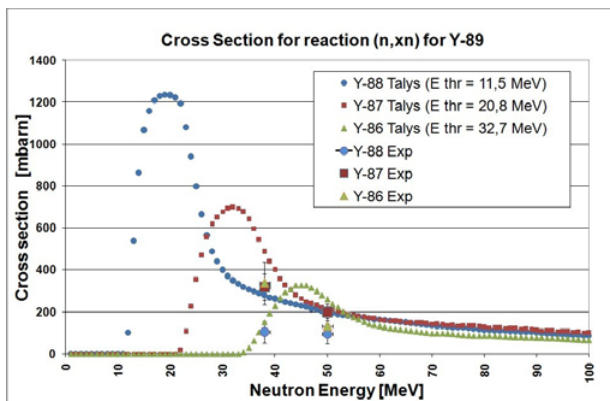


**Figure 5.** Comparison of  $^{89}\text{Y}$  (n,xn) cross-section measurements and calculations. Our Uppsala experiments in 2015 are represented by six bigger points. TALYS 1.8 [7] calculation results are represented by circles ( $^{88}\text{Y}$ ), squares ( $^{87}\text{Y}$ ) and triangles ( $^{86}\text{Y}$ ).

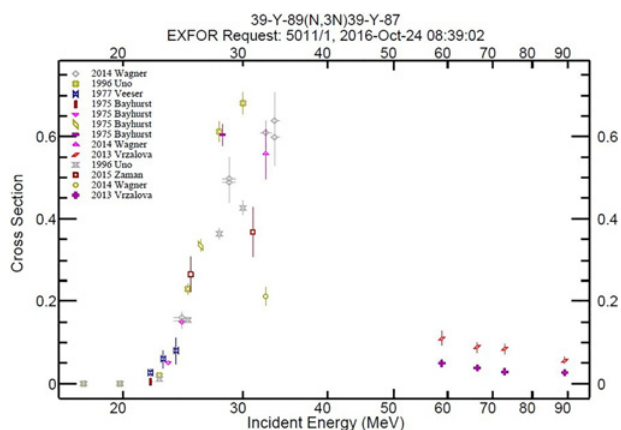


**Figure 6.** Cross-section for  $^{89}\text{Y}(n,3n)^{87}\text{Y}$  reaction from EXFOR data base. The last 4 double points for higher energy (on the right) are for production of  $^{87}\text{Y}$  in the ground state (the lower symbols) and in the isomeric state (the upper symbols) from Ref. [13].

$^{89}\text{Y}(n,4n)^{86}\text{Y}$  reaction there are no data sets in EXFOR. It means that those measurements are important and we will continue them in the near future. The comparison of our preliminary results with the available EXFOR data shows good applicability of used method of measurement and

data processing. We will continue analyzing our data and the calculation method (especially for higher energies, for which the data are not presented in this paper).

We would like to thank the personnel of TSL. Special thanks for M. Majerle for help. This experiment was supported by the EU FP7 CHANDA project, grant agreement No. 605203.

## References

- [1] E&T RAW— Collaboration, Communication of the JINR **E1-2010-61** (2010)
- [2] W. Furman, M. Bielewicz, S. Kilim, E. Strugalska-Gola, M. Szuta, A. Wojciechowski et al., PoS (Baldin ISHEPP XXI) **086**, [www.pos.sissa.it](http://www.pos.sissa.it) (2013)
- [3] J. Frana, Radioanal. and Nucl. Chem. **257**, 583 (2003)
- [4] M. Bielewicz, S. Kilim, E. Strugalska-Gola, M. Szuta, A. Wojciechowski, J. Korean Phys. Soc. **59**(2), 2014 (2011)
- [5] M. Bielewicz, E. Strugalska-Gola, M. Szuta, A. Wojciechowski et al., Nuclear Data Sheets **119**, 296–298 (2014)
- [6] Experimental Nuclear Reaction Data; EXFOR/CSISRS <https://www-nds.iaea.org/exfor/>
- [7] A.J. Koning, S. Hilaire, M.C. Duijvestijn; TALYS Santa Fe, AIP Conference Proceedings **769**, 1154–9 (2005)
- [8] A.V. Prokofiev, J. Blomgren et al., Uppsala, Sweden; Rad. Prot. Dosim. **126**, 18–22 (2007)
- [9] A.V. Prokofiev, E. Passoth, A. Hjalmarsson, and M. Majerle, IEEE Transactions on Nuclear Science **61**, 1929–1936 (2014)
- [10] I.O. Svoboda, Ph.D. Thesis, Czech Technical University in Prague (2011)
- [11] A.V. Prokofiev, M.B. Chadwick et al.; Journal of Nuclear Science and Technology, Suppl. 2 **1**, 112–115 (2002)
- [12] P. Chudoba, V. Wagner, J. Vrzalova, S. Kilim, M. Bielewicz, E. Strugalska-Gola, M. Szuta et al., Physics Procedia **59**, 114–118 (2014)
- [13] J. Vrzalova et al., Nuclear Instruments and Methods in Physics Research A **726**, 84–90 (2013)